Hybrid Interweave-Underlay Spectrum Access for Cognitive Cooperative Radio Networks

Thi My Chinh Chu, Hoc Phan, and Hans-Jürgen Zepernick, *Senior Member, IEEE*

***Abstract*—In this paper, we study a hybrid interweave-underlay spectrum access system that integrates amplify-and-forward relaying. In hybrid spectrum access, the secondary users flexibly switch between interweave and underlay schemes based on the state of the primary users. A continuous-time Markov chain is proposed to model and analyze the spectrum access mechanism of this hybrid cognitive cooperative radio network (CCRN). Utilizing the proposed Markov model, steady-state probabilities of spectrum access for the hybrid CCRN are derived. Furthermore, we assess performance in terms of outage probability, symbol error rate (SER), and outage capacity of this CCRN for Nakagami-m fading with integer values of fading severity parameter m. Numerical results are provided showing the effect of network parameters on the secondary network performance, such as the primary arrival rate, the distances from the secondary transmitters to the primary receiver, the interference power threshold of the primary receiver in underlay mode, and the average transmit signal-to-noise ratio of the secondary network in interweave mode. To show the performance improvement of the CCRN, comparisons for outage probability, SER, and capacity between the conventional underlay scheme and the hybrid scheme are presented. The numerical results show that the hybrid approach outperforms the conventional underlay spectrum access.**

***Index Terms*—Cognitive radio networks, continuous-time Markov chain, hybrid interweave-underlay, amplify-and-forward relaying, outage probability, symbol error rate, outage capacity.**

I. Introduction

NOWADAYS, the increasing demand on mobile multimedia leads to serious shortage of frequency spectrum. Despite this shortage, the allocated spectrum resources are still utilized inefficiently [1], which necessitates studies on efficient spectrum access mechanisms. Accordingly, cognitive radio technology has emerged as a promising approach to alleviate the insufficiency of spectrum utilization (see, e.g., [2]–[7], and the references therein). In the study of [2], the fundamental concepts for spectrum sharing have been featured. Furthermore, the work of [3] addressed several major functions of cognitive radios such as interference temperature estimation, spectrum hole detection, channel state estimation, transmit power control, and dynamic spectrum access.

Manuscript received April 11, 2013; revised August 30, 2013, January 17, 2014, and April 7, 2014; accepted May 7, 2014. Date of publication May 16, 2014; date of current version July 18, 2014. The editor coordinating the review of this paper and approving it for publication was H. Li.

T. M. C. Chu and H.-J. Zepernick are with the Blekinge Institute of Technology, 371 79 Karlskrona, Sweden (e-mail: thi.my.chinh.chu@bth.se; hans-jurgen.zepernick@bth.se).

H. Phan is with the School of Systems Engineering, University of Reading, Reading, RG6 6AY, U.K. (e-mail: h.phan@reading.ac.uk).

Digital Object Identifier 10.1109/TCOMM.2014.2325041

As for the spectrum access strategies, there exist three main approaches, i.e., the interweave, underlay, and overlay scheme [8]. In case of interweave spectrum access, secondary users (SUs) are not allowed to cause any interference to the primary network [3]. Therefore, an SU must periodically monitor the radio spectrum to detect spectrum occupancy and only opportunistically communicates over spectrum holes. This approach may reduce effectiveness of spectrum utilization. On the other hand, interweave spectrum access may offer superior system performance, such as outage probability and error probability, as compared to underlay and overlay networks given the same propagation environment [9]. This performance enhancement is attributed to the fact that transmit power of the SU is not bounded by an interference power constraint of the primary receiver. In addition, the received signal of the SU does not suffer from interference from the primary transmission. An alterative approach is known as underlay spectrum access wherein SUs and primary users (PUs) can simultaneously share the same licensed spectrum provided that the secondary transmit power is adjusted to meet the interference power constraint of the primary receiver [4]. Restricting transmit power leads to a significant reduction in channel capacity and radio coverage in the secondary network. On the other hand, effectiveness of spectrum utilization is improved with underlay spectrum access compared to the interweave scheme as spectrum can be utilized at any time. Finally, overlay spectrum access also allows the SUs to concurrently access spectrum with the PUs given that the SUs implement an appropriate technique to mitigate the interference to the primary network [6]. Interference mitigation in overlay spectrum access is based on SUs having knowledge about the primary network beyond spectrum occupancy but requires information such as code books or even messages that are communicated in the primary network.

Inspired by the inherent benefits of the above schemes, hybrid cognitive radio networks (CRNs) have been proposed as a means of improving the performance of secondary networks (see, for instance, [10], [11]). In [10], a novel hybrid scheme was introduced, which combines the conventional interweave and underlay schemes for a single hop CRN. Then, an M/M/1 queuing model with Poisson traffic generation is invoked to analyze the average service rate of SU video service. Furthermore, [11] proposed a power allocation strategy for a single hop hybrid overlay-underlay CRN to maximize channel capacity for the SU by using a suitable interference cancelation technique.

In addition, cooperative communications has been recently incorporated into CRNs aiming at improving system performance of secondary and/or primary networks [12]–[16]. In light of this, [14] proposed power and channel allocation strategies

for a cognitive cooperative radio network (CCRN) to optimize overall system throughput. Moreover, performance analysis in terms of outage probability and symbol error rate (SER) for multi-relay CCRNs was addressed in [15]. The use of cooperative communications in hybrid CRNs was studied in [16] in which the secondary users transmit with their power limits while the primary system is idle. However, when the primary system is active, the secondary users must control their transmit powers under the peak interference power constraint of the primary receiver. Nevertheless, the authors of [16] assumed that the probabilities for idle and active states of the primary transmitter are known and that the network suffers from Rayleigh fading when deriving a bound on the outage probability of the hybrid interweave-underlay CCRN. Thus, selection of operation mode in [16] does not take into account the traffic statistics of the primary and secondary network.

Apart from the aforementioned works, in this paper, we study the incorporation of hybrid interweave-underlay spectrum access into cognitive cooperative relay networks as a means of obtaining the inherent benefits of both hybrid interweave-underlay spectrum access as well as spatial diversity gains of cooperative communications. It is noted that, in our study, the traffic characteristics of both secondary and primary users are taken into consideration when modeling the investigated network as well as analyzing the corresponding system performance. Considering these stochastic processes, of course, covers a more general and practical setting as compared to [16]. Regarding the fading environments, it is assumed that the considered network is subject to Nakagami-m fading that will induce challenging expressions in the mathematical analysis. Nevertheless, this fading model comprises several other environments as special cases by setting the fading severity parameter m to a particular value, e.g., $m = 0.5$ represents a one-sided Gaussian distribution and $m = 1$ models Rayleigh fading. This general model also closely approximates Nakagami-q (Hoyt) fading and Nakagami-n (Rice) fading. Further, according to experimental and theoretical results, the Nakagami-m distribution is the best distribution for modeling urban multipath radio channels.

In order to achieving performance improvements, in our system, a secondary relay is used to assist the communication from a secondary transmitter to a secondary receiver. Clearly, integrating relay transmission into the secondary network as well as considering a more general fading model results in a demanding mathematical model and a complex analysis framework. On the other hand, our work gives a more general and practical setting of hybrid interweave-underlay cognitive networks as compared to [17]. In summary, major contributions of this paper can be stated as follows:

- We develop a Markov chain to model the dynamic behavior of the considered cognitive radio amplify-and-forward (AF) relay network with hybrid interweave-underlay spectrum access.
- On this basis, the equilibrium probability of each operation mode for the hybrid interweave-underlay cognitive relay system is derived.
- We further develop an analytical framework for evaluating system performance in terms of outage probability, SER, and outage capacity in case of Nakagami-m fading.

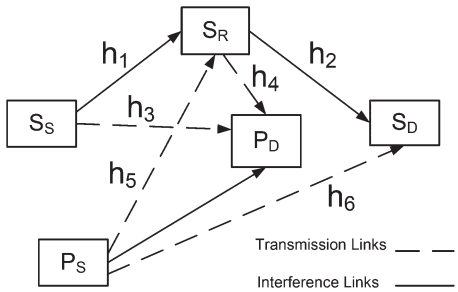

Fig. 1. System model of the hybrid interweave-underlay CCRN.

- We also make a performance comparison between the hybrid CCRN and a conventional cognitive radio network to reveal the superior performance of the hybrid cognitive relay scheme.
- Finally, through our analysis, insights into the impact of network parameters on system performance are revealed. In particular, we consider the impact of the primary arrival rate, the distances from the secondary transmitter to the primary receiver, fading parameters, the interference constraint threshold at the primary receiver in underlay mode, and the average transmit signal-to-noise ratio (SNR) in interweave mode.

The rest of the paper is organized as follows. Section II describes the system model for a hybrid interweave-underlay CCRN and adopts a Markov chain to model the reactions of the SUs to the PU's transmission. Steady-state probabilities, deduced from the Markov chain, are utilized to analyze system performance in Section III. Section IV provides numerical results. Finally, conclusions are given in Section V.

Notation: We use the following notations throughout the paper. The probability density function (PDF) and the cumulative distribution function (CDF) of a random variable (RV) X are denoted as $f_X(\cdot)$ and $F_X(\cdot)$, respectively. Here, $\Gamma(n)$ and $\Gamma(n, x)$ are the gamma function [18, eq. (8.310.1)] and the incomplete gamma function [18, eq. (8.350.2)], respectively. Next, the nth order modified Bessel function of the second kind [18, eq. (8.432.1)] is denoted as $\mathcal{K}_n(\cdot)$ and the Whittaker function [18, eq. (9.222)] is represented by $W_{a,b}(\cdot)$. Furthermore, ${}_2F_1(a, b; c; x)$ and $U(a, b; x)$ are, respectively, the Gauss hypergeometric function [18, eq. (9.100)] and confluent hypergeometric function [18, eq. (9.211.4)]. In addition, $\mathcal{B}(x, y)$ represents the beta function [18, eq. (8.380.1)] and $E\{\cdot\}$ stands for the expectation operator. Finally, $C_k^n = n!/(k!(n-k)!)$ is the binomial coefficient.

II. System and Channel Model

The CCRN that we consider consists of a primary source, $\mathrm{P_S}$, a primary destination, $\mathrm{P_D}$, a secondary source, $\mathrm{S_S}$, an AF relay, $\mathrm{S_R}$, and a secondary destination, $\mathrm{S_D}$ as depicted in Fig. 1. Here, h_1, h_2, h_3, h_4, h_5, and h_6 are, respectively, the channel coefficients of the links $\mathrm{S_S} \to \mathrm{S_R}$, $\mathrm{S_R} \to \mathrm{S_D}$, $\mathrm{S_S} \to \mathrm{P_D}$, $\mathrm{S_R} \to \mathrm{P_D}$, $\mathrm{P_S} \to \mathrm{S_R}$, and $\mathrm{P_S} \to \mathrm{S_D}$. Assume that the secondary transmission operates under Nakagami-m fading and in half-duplex mode, i.e., the secondary relaying transmission occurs in two time slots (TSs). In the first TS, $\mathrm{S_S}$ broadcasts a

signal while $\mathrm{S_R}$ amplifies the received signal with a scale factor and forwards it to $\mathrm{S_D}$ in the second TS.

In this system, we deploy hybrid spectrum access for the SUs where $\mathrm{S_S}$ and $\mathrm{S_R}$ flexibly switch between underlay and interweave mode based on the state of the PU. In particular, one TS of the hybrid cognitive transmission always consists of two phases, sensing phase and data transmission phase as in [19]. In the first phase, the SU, $\mathrm{S_S}$ or $\mathrm{S_R}$, listens to the spectrum allocated to the PU to detect the state of the PU. In the second phase, the SU adapts its transmit power based on the sensing results. If the spectrum is sensed idle in the first phase, taking advantage of not requiring the interference constraint, the SU operates in interweave mode with maximum transmit power $P_{\max}$. In contrast, if the PU is active, the SU must switch to underlay mode under the interference power constraint imposed by $\mathrm{P_D}$. Since sensing-based spectrum sharing for CRNs has been proposed in Section III.B of [19], in the context of our paper, we do not delve into spectrum sensing for the hybrid system anymore. Instead, we assume that the secondary users can perform perfect spectrum sensing as reported in Section III.B of [19].

It should be mentioned that in case of imperfect spectrum sensing, the cooperative sequential spectrum sensing approach can be employed where $\mathrm{S_S}$ and $\mathrm{S_R}$, $\mathrm{S_R}$ and $\mathrm{S_D}$ mutually exchange the sensing results. This approach essentially reduces the missed detection probability and the false alarm probability at each secondary user. Furthermore, given that the missed detection probability and the false alarm probability at each station can be driven to be lower than 0.1 as in [19], after cooperative sequential spectrum sensing, the missed detection and false alarm probabilities of the hybrid relay network are lower than 0.01. Then, the effect of imperfect spectrum sensing on the performance of the considered network may be neglected. It should also be mentioned that the sensing duration is often very small in the order of 1 ms as compared to the time slot duration of, say 100 ms. As such, the secondary users are considered in this work to start transmission at the beginning of each time slot with virtually no delay.

As for the implementation of the hybrid interweave-underlay CCRN, it should be mentioned that the scheme inherits the complexity from the interweave and underlay schemes. In particular, spectrum sensing must be implemented in each time slot and is compulsory for both interweave and hybrid schemes. In an interweave scheme, the SU keeps silent when the PU is active and only opportunistically transmits a signal when the PU does not occupy the spectrum. In a hybrid interweave-underlay CCRN, when the PU does not occupy the spectrum, the SU transmits its signals. However, when the spectrum is occupied by the PU, the SU is still allowed to transmit provided that its transmit power is continuously adapted under the interference power constraint imposed by the PU. Basically, instead of the SU turning off its transmit power when the PU occupies or starts occupying the spectrum, the hybrid CCRN switches to underlay mode. When the SUs operate in underlay mode, they must perform power adaptation under the interference power constraint of the PU. Therefore, the SUs need to obtain channel state information to the primary receivers to control their transmit powers. Thus, compared to the underlay scheme, the interweave-underlay scheme does not increase the complexity in power control when operating in underlay mode. In fact, the hybrid scheme is even simpler as it only must control its transmit power when the PU is active.

However, in some particular scenarios, it is not beneficial to deploy the hybrid spectrum access approach. For instance, when the secondary transmitters are rather far from the primary receiver such that, given a predefined transmit power range of the secondary transmitter, the interference power constraint of the primary receiver is often satisfied. In this case, the secondary network can operate freely in its transmit power range without considering the primary interference power constraint. On the contrary, for the case that the secondary transmitters are located close to the primary receiver, the transmit powers of the SUs in underlay spectrum access mode are severely constrained to be sufficiently low because of the interference power constraint of the primary receiver. Then, the SUs may take advantage of the interweave spectrum access, i.e., not suffering from the interference power constraint when the licensed bands are not occupied by the PU. In this scenario, it is beneficial to apply the hybrid scheme as it not only allows the secondary network to access the spectrum at any time but can also offer performance improvements when opportunistically operating in interweave mode.

In this paper, we apply the hybrid spectrum access scheme for the scenario that the secondary transmitter is located close to the primary receiver. Let X_3 be a random variable which represents the channel power gain of the link from the secondary transmitter to the primary receiver. With the predefined interference power constraint Q of the primary receiver and transmit power limit $P_{\max}$ of the secondary transmitter, the transmit power of the secondary transmitter in underlay mode is controlled as $\min\{Q/X_3, P_{\max}\}$. However, when the secondary transmitter is rather close to the primary receiver, the probability of the event $Q/X_3 > P_{\max}$ is very low, i.e., the constraint of $P_{\max}$ on the transmit power of the secondary user in underlay mode can be neglected. In this case, the transmit power of the SU in underlay mode is considered to be only constrained by the interference power threshold Q as in [4], [20].

To assess the system performance of the hybrid scheme, we need to obtain the probabilities that the cognitive relay system operates in interweave mode and underlay mode. To solve this issue, it is necessary to propose a suitable model to capture the system dynamics, especially the effect of the PU activities on the selection of operation mode for the SUs. It should be mentioned that the active/inactive periods of PUs are typically much larger than the duration of one time slot [21]. Thus, we can make the assumption that the TS is sufficiently small as compared to the average arrival period of packets. Then, the states of the primary and secondary users can be considered to change continuously over time units of a TS. Assume that the arrival traffics of the primary and secondary systems are modeled as Poisson random processes and that spectrum access durations or departure times of PUs and SUs are negative-exponentially distributed. As in [9], [17], [22], if arrival and departure traffics are Poisson processes, the spectrum access can be modeled as a continuous-time Markov chain (CTMC).

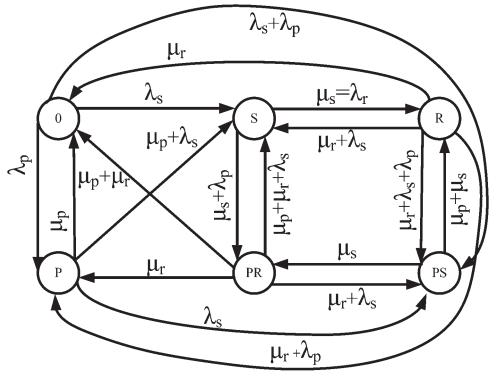

Fig. 2. Continuous-time Markov chain with six states modeling the spectrum access of the hybrid interweave-underlay CCRN.

Let the arrival traffic of $\mathrm{P_S}$ be modeled as a Poisson process with arrival rate λ_p packets/TS and let the departure traffic of $\mathrm{P_S}$ be another Poisson process with departure rate μ_p packets/TS. Furthermore, the arrival and departure traffics of $\mathrm{S_S}$ and $\mathrm{S_R}$ shall be modeled as Poisson processes with rates λ_s, μ_s, and λ_r, μ_r packets/TS, respectively. In this CCRN, all departure packets of $\mathrm{S_S}$ become arrival packets of $\mathrm{S_R}$, i.e., $\mu_s = \lambda_r$. Recall that transmissions of $\mathrm{S_S}$ and $\mathrm{S_R}$ always occur in different TSs, as is the common case for cooperative communications. Thus, the probability of $\mathrm{S_S}$ and $\mathrm{S_R}$ simultaneously transmitting signals is equal to zero. We assume that $\mathrm{S_S}$ and $\mathrm{S_R}$ do not change their operation mode in a time slot, i.e., the system does not change its state during a TS. Even when the primary user requires service during the transmission period of the secondary user, $\mathrm{S_S}$ or $\mathrm{S_R}$ still keep the operation mode in the current time slot but adapt their operation modes in the next slot, i.e., the system may change its state in a subsequent TS. This assumption is based on the duration of a time slot being rather short and the probability of the event that a primary user requires service in the middle of a secondary time slot is very small for independent Poisson processes [17]. As such, the effect of the secondary network remaining in its operation mode during a time slot on the performance of the primary network can be neglected. As a result, the spectrum access of this hybrid interweave-underlay CCRN can be modeled as a six state continuous-time Markov chain as shown in Fig. 2.

In the state diagram of the Markov chain shown in Fig. 2, State 0 represents the state that all terminals $\mathrm{P_S}$, $\mathrm{S_S}$, $\mathrm{S_R}$ are idle. States P, S, R correspond to the states that only $\mathrm{P_S}$, only $\mathrm{S_S}$, only $\mathrm{S_R}$ operate, respectively. Finally, States PS and PR stand for the states that both $\mathrm{P_S}$ and $\mathrm{S_S}$, and both $\mathrm{P_S}$ and $\mathrm{S_R}$ are active, respectively. It can be easily seen that this continuous-time Markov chain converges to a steady-state distribution because it possesses two sufficient conditions for convergence [23, p. 263]. First, the proposed continuous-time Markov chain has a finite state space with six states: $\{0, \mathrm{S}, \mathrm{R}, \mathrm{PR}, \mathrm{PS}, \mathrm{P}\}$. Secondly, this continuous-time Markov chain is irreducible because every state of the Markov chain can be reached from other states.

Without loss of generality, it is assumed that the network is initialized as inactive, i.e., the Markov chain resides in State 0. Upon the first access effort of the secondary transmitter, $\mathrm{S_S}$, the Markov chain goes from State 0 to State S with transition rate λ_s. Since only $\mathrm{S_S}$ occupies the spectrum, it will operate in interweave mode, i.e., not face the interference power constraint from the primary user. As long as transmission of $\mathrm{S_S}$ ends before $\mathrm{P_S}$ requests to use the spectrum, the system goes from State S to State R with transition rate μ_s. Because the departure traffic of the secondary transmitter, $\mathrm{S_S}$, becomes the arrival traffic with rate λ_r of the secondary relay, $\mathrm{S_R}$, we have $\lambda_r = \mu_s$. Then, $\mathrm{S_R}$ will operate in interweave mode in which only $\mathrm{S_R}$ utilizes the spectrum in the second time slot. If $\mathrm{S_R}$ completes its communication before a spectrum access of $\mathrm{S_S}$ or $\mathrm{P_S}$ occurs, the system transits from State R to State 0 with rate μ_r. Otherwise, the system will transit from state R to P with rate $\mu_r + \lambda_p$, from state R to S with rate $\mu_r + \lambda_s$, or from state R to PS with rate $\mu_r + \lambda_s + \lambda_p$.

It is noted that the probability of the transition from state R to P corresponds to the joint probability of two Poisson processes occuring, i.e., $\mathrm{S_R}$ completes its communication with rate μ_r and there is an arrival of the primary user with rate λ_p in the current TS. It is also well known that the sum of two independent Poisson random variables results in a Poisson random variable whose transition rate is equal to the summation of the two rates. Thus, the system transits from state R to P with rate $\mu_r + \lambda_p$. A similar line of argument can be utilized to explain the transitions from state R to S with rate $\mu_r + \lambda_s$, or from state R to PS with rate $\mu_r + \lambda_s + \lambda_p$.

When the system resides in State S, i.e., $\mathrm{S_S}$ is transmitting in interweave mode, if the primary user $\mathrm{P_S}$ requests the spectrum, the system transits from State S to State PR with transition rate $\mu_s + \lambda_p$ at the end of this time slot. At State PR, both $\mathrm{S_R}$ and $\mathrm{P_S}$ simultaneously operate in the spectrum. Therefore, $\mathrm{S_R}$ must switch to underlay mode in the second time slot subject to the interference power constraint imposed by $\mathrm{P_D}$. Once $\mathrm{S_R}$ completes its communication at the end of the second time slot, depending on the arrival and departure processes of the users during this time slot, the system will make one of the following transitions: A transition from State PR to State P with transition rate μ_r, from State PR to State 0 with transition rate $\mu_r + \mu_p$, from State PR to State PS with transition rate $\mu_r + \lambda_s$, or from State PR to State S with transition rate $\mu_r + \mu_p + \lambda_s$. It is noted that the transition from State P to State PS is assumed to occur with rate λ_s, instead of $\lambda_s + \lambda_p$. This implicitly corresponds to the event that the primary user is active in the current time slot and still remains active in the subsequent time slot. Similarly, we can explain all remaining transitions that are shown in Fig. 2.

Let p_0, p_p, p_s, p_r, p_{ps}, and p_{pr} denote the steady-state probabilities for States 0, P, S, R, PS, and PR in the proposed Markov chain, respectively. The steady-state probability of each state can be derived based on the flow-balance equations at all nodes of the Markov chain, which states that the arrival rate of any node is always equal to its departure rate, and the normalized equation, which implies that the total probabilities of all states is always equal to one. Consequently, the steady-state probabilities of the six states can be obtained from a linear equation system as in (1), shown at the bottom of the next page.

It is sufficient to select six independent equations from (1) to obtain six steady-state probabilities. From (1), we can

express the first five flow-balance equations and the normalized equation as $\mathbf{Ap} = \mathbf{b}$. Here, $\mathbf{p}$ is a column vector $\mathbf{p} = [p_0, p_p, p_s, p_r, p_{ps}, p_{pr}]^T$ which represents the steady-state probabilities of the six above states. Furthermore, $\mathbf{b}$ is a column vector defined as $\mathbf{b} = [0, 0, 0, 0, 0, 1]^T$ and $\mathbf{A}$ denotes a 6×6 matrix constructed as in (2), shown at the bottom of the page.

Thus, the six steady-state probabilities $p_0, p_p, p_s, p_r, p_{ps}$, and p_{pr} are found as $\mathbf{p} = \mathbf{A}^{-1}\mathbf{b}$. As a result, the probability p that the secondary transmission occurs is given by the probability that $\mathrm{S_S}$ is active in the first TS and $\mathrm{S_R}$ is active in the second TS, i.e., p can be calculated as

$$p = (p_s + p_{ps})(p_r + p_{pr}) \tag{3}$$

We assume that the secondary users, $\mathrm{S_S}$ and $\mathrm{S_R}$, do not change their operation mode during a time slot but instead adapt the operation mode in the subsequent time slot. Based on the current state at the beginning of each time slot, the secondary user decides whether interweave or underlay mode should be deployed for each TS. When the system is in State S or R, $\mathrm{S_S}$ or $\mathrm{S_R}$ operates in interweave mode. During periods of States PS and PR, $\mathrm{S_S}$ and $\mathrm{S_R}$ must operate in underlay mode. Therefore, there are four scenarios to be distinguished for the transmission modes of the hybrid interweave-underlay AF relay system as follows:

- *Scenario 1:* $\mathrm{P_S}$ is active in both TSs of the secondary transmission.
- *Scenario 2:* $\mathrm{P_S}$ is only active in the first TS of the secondary transmission.
- *Scenario 3:* $\mathrm{P_S}$ is only active in the second TS of the secondary transmission.
- *Scenario 4:* $\mathrm{P_S}$ is inactive in both TSs of the secondary transmission.

Let x_i, $i \in \{1, 2, 3, 4\}$, be the transmit symbol at $\mathrm{S_S}$ with average power $P_{s,i}$ and n_0 is additive white Gaussian noise (AWGN) with zero-mean and variance N_0 at $\mathrm{S_R}$ and $\mathrm{S_D}$. Further, we denote $y_{r,i}$ and $y_{d,i}$, respectively, as the received signals at $\mathrm{S_R}$ and $\mathrm{S_D}$ in Scenario i. Finally, G_i stands for the gain factor at $\mathrm{S_R}$ in Scenario i. It is assumed that the noise power at the secondary relay $\mathrm{S_R}$ is much lower than its received signal power. Therefore, we can neglect the noise power at $\mathrm{S_R}$ when calculating the gain factor G_i. In what follows, we derive the gain factors and the expressions of the instantaneous SNR as well as the signal-to-interference plus noise ratio (SINR) for all possible scenarios.

Scenario 1: $\mathrm{P_S}$ is active in both TSs of the secondary transmission. The probability that this scenario occurs is

$$p_1 = \frac{p_{ps}p_{pr}}{(p_s + p_{ps})(p_r + p_{pr})} \tag{4}$$

The received signal $y_{r,1}$ at $\mathrm{S_R}$ in Scenario 1 is obtained as

$$y_{r,1} = h_1 x_1 + h_5 x_p + n_0 \tag{5}$$

where n_0 is AWGN with zero-mean and variance N_0 at $\mathrm{S_R}$. In addition, x_p is the transmit signal of the primary transmitter $\mathrm{P_S}$, and $h_5 x_p$ is the interference from $\mathrm{P_S}$ to $\mathrm{S_R}$. As in [24], [25], the interference distribution in wireless networks can be approximated as a Gaussian distribution. Thus, we approximate the effect of interference and noise at the relay $h_5 x_p + n_0$ as another Gaussian random variable n_r with zero-mean and variance N_r where N_r is calculated based on the power law decaying path-loss plus the noise at the relay. Then, the received signal at the secondary destination is

$$y_{d,1} = G_1 h_2 (h_1 x_1 + n_r) + h_6 x_p + n_0 \tag{6}$$

$$\begin{aligned}
&-(2\lambda_s + 2\lambda_p)p_0 + \mu_p p_p + 0p_s + \mu_r p_r + 0p_{ps} + (\mu_r + \mu_p)p_{pr} = 0\\
&\lambda_p p_0 - (2\mu_p + 2\lambda_s)p_p + 0p_s + (\mu_r + \lambda_p)p_r + 0p_{ps} + \mu_r p_{pr} = 0\\
&\lambda_s p_0 + (\mu_p + \lambda_s)p_p - (2\mu_s + \lambda_p)p_s + (\mu_r + \lambda_s)p_r + 0p_{ps} + (\mu_p + \mu_r + \lambda_s)p_{pr} = 0\\
&0p_0 + 0p_p + \mu_s p_s - (4\mu_r + 2\lambda_p + 2\lambda_s)p_r + (\mu_s + \mu_p)p_{ps} + 0p_{pr} = 0\\
&(\lambda_p + \lambda_s)p_0 + \lambda_s p_p + 0p_s + (\mu_r + \lambda_p + \lambda_s)p_r - (2\mu_s + \mu_p)p_{ps} + (\mu_r + \lambda_s)p_{pr} = 0\\
&0p_0 + 0p_p + (\mu_s + \lambda_p)p_s + \mu_s p_{ps} - (2\mu_p + 4\mu_r + 2\lambda_s)p_{pr} = 0\\
&p_0 + p_p + p_s + p_r + p_{ps} + p_{pr} = 1
\end{aligned} \tag{1}$$

$$\mathbf{A} = \begin{pmatrix}
-(2\lambda_s + 2\lambda_p) & \mu_p & 0 & \mu_r & 0 & (\mu_r + \mu_p)\\
\lambda_p & -(2\mu_p + 2\lambda_s) & 0 & \mu_r + \lambda_p & 0 & \mu_r\\
\lambda_s & \mu_p + \lambda_s & -(2\mu_s + \lambda_p) & \mu_r + \lambda_s & 0 & \mu_p + \mu_r + \lambda_s\\
0 & 0 & \mu_s & -(4\mu_r + 2\lambda_p + 2\lambda_s) & \mu_s + \mu_p & 0\\
(\lambda_p + \lambda_s) & \lambda_s & 0 & (\mu_r + \lambda_p + \lambda_s) & -(\mu_p + 2\mu_s) & \mu_r + \lambda_s\\
1 & 1 & 1 & 1 & 1 & 1
\end{pmatrix} \tag{2}$$

where n_0 is AWGN with zero-mean and variance N_0 at $\mathrm{S_D}$ and $h_6 x_p$ is the interference from $\mathrm{P_S}$ to $\mathrm{S_R}$. Again, $h_6 x_p + n_0$ is approximated as another Gaussian random variable n_d with zero-mean and variance N_d, i.e.,

$$y_{d,1} = G_1 h_2 h_1 x_1 + G_1 h_2 n_r + n_d \tag{7}$$

In this scenario, both $\mathrm{S_S}$ and $\mathrm{S_R}$ operate in underlay mode under the interference power constraint Q of $\mathrm{P_D}$. Thus, the average transmit power $P_{s,1}$ of $\mathrm{S_S}$ and the average transmit power $P_{r,1}$ of $\mathrm{S_R}$ must be regulated to meet the interference threshold Q of $\mathrm{P_D}$, i.e., $P_{s,1} = E\{|x_1|^2\} = Q/|h_3|^2$ and $P_{r,1} = E\{|G_1 h_1 x_1|^2\} = Q/|h_4|^2$. Here, h_3 and h_4 are the channel coefficients of the links $\mathrm{S_S} \to \mathrm{P_D}$ and $\mathrm{S_R} \to \mathrm{P_D}$, respectively. Let X_1, X_2, X_3, X_4 be the channel power gains of the links $\mathrm{S_S} \to \mathrm{S_R}$, $\mathrm{S_R} \to \mathrm{S_D}$, $\mathrm{S_S} \to \mathrm{P_D}$, $\mathrm{S_R} \to \mathrm{P_D}$, respectively, i.e., $X_i = |h_i|^2$, $i \in \{1, 2, 3, 4\}$. Thus, the gain factor G_1 at $\mathrm{S_R}$ in Scenario 1 is selected as

$$G_1^2 = \frac{X_3}{X_1 X_4} \tag{8}$$

Defining $\beta_1 = Q/N_r$ and $\beta_2 = Q/N_d$, the SINR γ_1 of the secondary system in Scenario 1 can be obtained as

$$\gamma_1 = \frac{\beta_1 \beta_2 X_1 X_2}{\beta_1 X_1 X_4 + \beta_2 X_2 X_3} \tag{9}$$

Scenario 2: $\mathrm{P_S}$ is active in the first TS and idle in the second TS of the secondary transmission. The probability that this scenario takes place is

$$p_2 = \frac{p_{ps} p_r}{(p_s + p_{ps})(p_r + p_{pr})} \tag{10}$$

Accordingly, the received signal $y_{d,2}$ at the secondary destination $\mathrm{S_D}$ in Scenario 2 is obtained as

$$y_{d,2} = G_2 h_2 h_1 x_2 + G_2 h_2 n_r + n_0 \tag{11}$$

Since $\mathrm{P_S}$ is active in the first TS and idle in the second TS of the secondary transmission, $\mathrm{S_S}$ operates in underlay mode with average transmit power $P_{s,2} = E\{|x_2|^2\} = Q/X_3$ in the first TS. However, $\mathrm{S_R}$ operates in interweave mode with average transmit power $P_{r,2} = E\{|G_2 h_1 x_2|^2\} = P_{\max}$ in the second TS. Then, the gain factor G_2 at $\mathrm{S_R}$ in Scenario 2 is chosen as

$$G_2^2 = \frac{P_{\max} X_3}{Q X_1} \tag{12}$$

Hence, the instantaneous SINR γ_2 at $\mathrm{S_D}$ in Scenario 2 is given by

$$\gamma_2 = \beta_1 \frac{X_1 X_2}{X_2 X_3 + \beta_3 X_1} \tag{13}$$

where $\beta_3 = Q/(P_{\max} N_r)$.

Scenario 3: $\mathrm{P_S}$ is idle in the first TS and active in the second TS of the secondary transmission. The probability of this scenario is

$$p_3 = \frac{p_s p_{pr}}{(p_s + p_{ps})(p_r + p_{pr})} \tag{14}$$

In this scenario, the received signal $y_{d,3}$ at the secondary destination $\mathrm{S_D}$ is given as

$$y_{d,3} = G_3 h_2 h_1 x_3 + G_3 h_2 n_0 + n_d \tag{15}$$

Because $\mathrm{P_S}$ is idle in the first TS of the secondary transmission, $\mathrm{S_S}$ operates in interweave mode with average transmit power $P_{s,3} = E\{|x_3|^2\} = P_{\max}$ in the first TS. However, since $\mathrm{P_S}$ is active in the second TS of the secondary transmission, $\mathrm{S_R}$ operates in underlay mode in the second TS under the interference power constraint Q, i.e., $P_{r,3} = E\{|G_3 h_1 x_3|^2\} = Q/X_4$. Thus, in Scenario 3, the gain factor G_3 at $\mathrm{S_R}$ is chosen as

$$G_3^2 = \frac{Q}{P_{\max} X_1 X_4} \tag{16}$$

Then, the instantaneous SINR γ_3 at $\mathrm{S_D}$ in Scenario 3 can be expressed as

$$\gamma_3 = \beta_2 \frac{X_1 X_2}{X_1 X_4 + \beta_4 X_2} \tag{17}$$

where $\beta_4 = N_0 Q/(N_d P_{\max})$.

Scenario 4: $\mathrm{P_S}$ is inactive in both TSs of the secondary transmission. The probability that Scenario 4 happens is

$$p_4 = \frac{p_s p_r}{(p_s + p_{ps})(p_r + p_{pr})} \tag{18}$$

Accordingly, the received signal at $\mathrm{S_D}$ is expressed as

$$y_{d,4} = G h_2 h_1 x_4 + G h_2 n_0 + n_0 \tag{19}$$

In this scenario, both $\mathrm{S_S}$ and $\mathrm{S_R}$ operate in interweave mode with average transmit power $P_{\max}$. Thus, the gain factor G_4 is chosen as for the conventional relay system, i.e.,

$$G_4^2 = 1/X_1 \tag{20}$$

Consequently, the instantaneous SNR γ_4 at $\mathrm{S_D}$ in Scenario 4 can be found as in conventional AF relay systems as

$$\gamma_4 = \beta_5 \frac{X_1 X_2}{X_1 + X_2} \tag{21}$$

where $\beta_5 = P_{\max}/N_0$.

In order to support the subsequent performance analysis, we provide the CDF and PDF of X_i, $i \in \{1, 2, 3, 4\}$, for a Nakagami-m fading channel with channel mean power Ω_i and positive integer values of fading severity m_i as

$$f_{X_i}(x_i) = \frac{\alpha_i^{m_i}}{\Gamma(m_i)} x_i^{m_i - 1} \exp(-\alpha_i x_i) \tag{22}$$

$$F_{X_i}(x_i) = 1 - \exp(-\alpha_i x_i) \sum_{j=0}^{m_i - 1} \frac{\alpha_i^j x_i^j}{j!} \tag{23}$$

where $\alpha_i = m_i/\Omega_i$.

III. End-to-End Performance Analysis

In general, the expectation $\overline{B}$ of a specific performance metric B can be formulated as in [21]

$$\overline{B} = \lim_{T\to\infty} \frac{1}{T} E\left[\int_0^T B(t)dt\right] \tag{24}$$

where $B(t)$ is the performance metric of the system at time instant t. For a discrete state space A, we have

$$\overline{B} = \sum_{i\in A} B(i)p_i \tag{25}$$

where i denotes any state in A, $B(i)$ is the average performance metric of the system in State i and p_i represents the probability that the system falls into State i.

A. Outage Probability Performance

Outage probability is defined as the probability that the instantaneous SNR falls below a predefined threshold γ_{th}. Applying (25) to the hybrid interweave-underlay CCRN, this metric can be obtained as

$$P_{out} = \sum_{i=1}^{4} p_i P_{i,out} \tag{26}$$

where p_i, $i \in \{1,2,3,4\}$, is the probability that Scenario i applies and $P_{i,out} = F_{\gamma_i}(\gamma_{th})$ is the outage probability in Scenario i. Hence, our goal is to derive the CDFs of the instantaneous SINRs for Scenarios 1, 2, 3, and the instantaneous SNR for Scenario 4.

Scenario 1: In view of (9), the CDF of the instantaneous SINR γ_1 for Scenario 1 can be expressed as (27). With the expression of $f_{X_i}(x_i)$ in (22) along with the help of [18, eq. (3.381.4)], I can be simplified as

$$I = 1 - \sum_{q=0}^{m_2-1} \frac{\beta_2^{m_4}\alpha_2^q\alpha_4^{m_4}}{q!}\frac{\Gamma(m_4+q)}{\Gamma(m_4)}\frac{\gamma^q}{(\alpha_2\gamma+\beta_2\alpha_4)^{m_4+q}} \tag{28}$$

We can rewrite the inner integral I_1 given in (27) as

$$I_1 = \frac{1}{\beta_1\beta_2}\int_0^\infty F_{X_1}\left(\frac{\gamma x_3}{\beta_1} + \frac{\gamma^2 x_3 x_4}{x_2}\right) f_{X_2}\left(\frac{x_2+\gamma\beta_1 x_4}{\beta_1\beta_2}\right) dx_2 \tag{29}$$

Substituting (22) and (23) into (29) and then using [18, eq. (3.471.9)] to calculate the remaining integral, after some manipulations, an expression for I_1 can be written as (30) at the bottom of the page. Using (30) and (22) together with the help of [18, eq. (6.643.3)], we can obtain an expression for I_2 as

$$\begin{aligned} I_2 = 1 - F_{X_2}\left(\frac{\gamma x_4}{\beta_2}\right) - \sum_{p=0}^{m_1-1}\sum_{q=0}^{p}\frac{C_q^p}{p!}\sum_{r=0}^{m_2-1} C_r^{m_2-1}\Gamma(m_3+p) \\ \times \frac{\Gamma(m_3+p+r-q+1)}{\Gamma(m_2)\Gamma(m_3)} \\ \times \frac{\beta_1^{m_3}\alpha_1^{(2p+r-q)/2}\alpha_2^{(2m_2-r+q-2)/2}\alpha_3^{m_3}}{\beta_2^{(2m_2-r+q-2)/2}} \end{aligned}$$

$$F_{\gamma_1}(\gamma) = \underbrace{\int_0^\infty\int_0^\infty\int_0^{\gamma x_4/\beta_2} f_{X_2}(x_2)f_{X_3}(x_3)f_{X_4}(x_4)dx_2dx_3dx_4}_{I} + \underbrace{\int_0^\infty \underbrace{\left(\int_0^\infty \underbrace{\left(\int_{\gamma x_4/\beta_2}^\infty F_{X_1}\left(\frac{\gamma x_2 x_3}{\beta_1 x_2 - \gamma x_4}\right) f_{X_2}(x_2)dx_2\right)}_{I_1}\right)}_{I_2} f_{X_3}(x_3)dx_3\right)}_{I_3} f_{X_4}(x_4)dx_4 \tag{27}$$

$$I_1 = 1 - F_{X_2}\left(\frac{\gamma x_4}{\beta_2}\right) - 2\sum_{p=0}^{m_1-1}\sum_{q=0}^{p} C_q^p \sum_{r=0}^{m_2-1}\frac{C_r^{m_2-1}\gamma^{m_2+p}}{p!\,\Gamma(m_2)}\frac{\alpha_1^{(2p+r-q+1)/2}\alpha_2^{(2m_2-r+q-1)/2}x_3^{(2p+r-q+1)/2}x_4^{(2m_2+q-r-1)/2}}{\beta_1^{(2p+r-q+1)/2}\beta_2^{(2m_2-r+q-1)/2}} \times \exp\left(-\frac{\alpha_1\gamma x_3}{\beta_1}\right)\exp\left(-\frac{\alpha_2\gamma x_4}{\beta_2}\right)\mathcal{K}_{r-q+1}\left(2\sqrt{\frac{\alpha_1\alpha_2\gamma^2 x_3 x_4}{\beta_1\beta_2}}\right) \tag{30}$$

$$\times \frac{\gamma^{m_2+p-1} x_4^{(2m_2+q-r-2)/2}}{(\alpha_1\gamma+\beta_1\alpha_3)^{(2m_3+2p+r-q)/2}} \times \exp\left(-\frac{\gamma^2\alpha_1\alpha_2+2\alpha_2\gamma\beta_1\alpha_3}{2\beta_2(\alpha_1\gamma+\beta_1\alpha_3)}x_4\right) \times W_{-\frac{2m_3+2p+r-q}{2},\frac{r-q+1}{2}}\left(\frac{\gamma^2\alpha_1\alpha_2 x_4}{\beta_2(\alpha_1\gamma+\beta_1\alpha_3)}\right) \quad (31)$$

Having the expression of I_2 in (31) and $f_{X_3}(x_3)$ in (22), we can reach an expression for the outer integral I_3 through the help of [18, eq. (7.621.3)]. Substituting this outcome and (28) into (27), then utilizing [18, eq. (7.621.3)] to solve the remaining integral, after rearranging terms, the CDF of the instantaneous SINR for Scenario 1 can be formulated as

$$F_{\gamma_1}(\gamma) = 1 - \sum_{p=0}^{m_1-1}\frac{1}{p!}\sum_{q=0}^{p} C_q^p \sum_{r=0}^{m_2-1} C_r^{m_2-1}\frac{\Gamma(m_4+m_2)}{\Gamma(m_2)\Gamma(m_3)} \times \frac{\Gamma(m_3+p+r-q+1)\Gamma(m_4+m_2+q-r-1)\beta_1^{m_3}}{\Gamma(m_4)\Gamma(m_4+m_3+m_2+p)} \times \frac{\Gamma(m_3+p)\alpha_1^{p+r-q+1}\alpha_2^{m_2}\alpha_3^{m_3}\alpha_4^{m_4}\beta_2^{m_4}\gamma^{m_2+p+r-q+1}}{(\alpha_2\gamma+\beta_2\alpha_4)^{m_4+m_2}(\alpha_1\gamma+\beta_1\alpha_3)^{m_3+p+r-q+1}} \times {}_2F_1\left(m_4+m_2, m_3+p+r-q+1, m_4+m_3+m_2+p; \frac{\beta_2\alpha_1\alpha_4\gamma+\beta_1\alpha_2\alpha_3\gamma+\beta_1\beta_2\alpha_3\alpha_4}{\alpha_1\alpha_2\gamma^2+\beta_2\alpha_1\alpha_4\gamma+\beta_1\alpha_2\alpha_3\gamma+\beta_1\beta_2\alpha_3\alpha_4}\right) \quad (32)$$

Similarly, we can derive the CDFs of the instantaneous SINRs for Scenarios 2, 3, and the instantaneous SNR for Scenario 4 as follows:

Scenario 2:

$$F_{\gamma_2}(\gamma) = 1 - \sum_{p=0}^{m_1-1}\sum_{q=0}^{p}\frac{C_q^p}{p!}\sum_{i=0}^{m_2-1} C_i^{m_2-1}\beta_1^{(2m_3-2m_2+i-q+2)/2} \times \frac{\beta_3^{(2m_2+q-i-2)/2}\alpha_2^{(2m_2+q-i-2)/2}\alpha_3^{m_3}}{\alpha_1^{m_3}(\gamma+\beta_1\alpha_3/\alpha_1)^{(2m_3+2p+i-q)/2}} \times \frac{\Gamma(m_3+p)\gamma^{m_2+p-1}}{\Gamma(m_2)}\frac{\Gamma(m_3+p+i-q+1)}{\Gamma(m_3)} \times \exp\left(-\frac{\alpha_1\alpha_2\gamma^2\beta_3+2\alpha_2\alpha_3\gamma\beta_3\beta_1}{2\beta_1(\alpha_1\gamma+\beta_1\alpha_3)}\right) \times W_{-\frac{2m_3+2p+i-q}{2},\frac{i-q+1}{2}}\left(\frac{\alpha_1\alpha_2\beta_3\gamma^2}{\beta_1(\alpha_1\gamma+\beta_1\,\alpha_3)}\right) \quad (33)$$

Scenario 3:

$$F_{\gamma_3}(\gamma_3) = 1 - \sum_{p=0}^{m_1-1}\sum_{q=0}^{p}\frac{C_q^p}{p!}\sum_{i=0}^{m_2-1} C_i^{m_2-1}\alpha_1^{(2p+i-q)/2}\alpha_4^{m_4} \times \frac{\beta_2^{(2m_4-2p+q-i)/2}\beta_4^{(2p+i-q)/2}\Gamma(m_4+m_2+q-i-1)}{\alpha_2^{m_4}\Gamma(m_2)\Gamma(m_4)(\gamma+\alpha_4\beta_2/\alpha_2)^{(2m_4+2m_2+q-i-2)/2}} \times \Gamma(m_4+m_2)\gamma^{m_2+p-1}\exp\left(-\frac{\alpha_1\beta_4\gamma(\alpha_2\gamma+2\alpha_4\beta_2)}{2\beta_2(\alpha_2\gamma+\alpha_4\beta_2)}\right) \times W_{-\frac{2m_4+2m_2+q-i-2}{2},\frac{i-q+1}{2}}\left(\frac{\alpha_1\alpha_2\gamma^2\beta_4}{\beta_2(\alpha_2\gamma+\alpha_4\beta_2)}\right) \quad (34)$$

Scenario 4:

$$F_{\gamma_4}(\gamma) = 1 - 2\sum_{p=0}^{m_1-1}\sum_{q=0}^{p}\frac{C_q^p}{p!}\sum_{i=0}^{m_2-1}\frac{C_i^{m_2-1}\alpha_1^{\frac{2p+i-q+1}{2}}\gamma^{m_2+p}}{\Gamma(m_2)\beta_5^{m_2+p}} \times \alpha_2^{\frac{2m_2-i+q-1}{2}}\exp(-\alpha_1\gamma+\alpha_2\gamma\beta_5)\mathcal{K}_{i-q+1}\left(2\sqrt{\frac{\alpha_1\alpha_2\gamma^2}{\beta_5^2}}\right) \quad (35)$$

Using γ_{th} as the argument of (32)–(35), we obtain $P_{i,out} = F_{\gamma_i}(\gamma_{th})$, $i \in \{1,2,3,4\}$. By substituting these outcomes into (26), finally, the outage probability for the secondary transmission is found.

B. SER Performance

Using (25) for the hybrid interweave-underlay CCRN, the SER can be obtained as

$$P_E = \sum_{i=1}^{4} p_i P_{i,E} \quad (36)$$

where $P_{i,E}$ is the SER for Scenario i. For each scenario, the SER can be expressed in terms of the instantaneous SINR (or SNR in Scenario 4) γ_i as in [26]

$$P_{i,E} = \frac{a\sqrt{b}}{2\sqrt{\pi}}\int_0^\infty F_{\gamma_i}(\gamma)\gamma^{-\frac{1}{2}}e^{-b\gamma}d\gamma \quad (37)$$

where a and b are modulation parameters. Since it is too complicated to derive expressions for the SERs of Scenarios 1, 2, and 3 directly from the exact expressions of the CDFs of the instantaneous SINRs γ_1 in (32), γ_2 in (33), and γ_3 in (34), we instead utilize the CDFs of the bounds on γ_1, γ_2, and γ_3 to obtain approximations for the SERs. Applying [27, eq. (25)] and [28, eq. (2)] to (9), (13), and (17), bounds γ_1^u, γ_2^u, and γ_3^u on γ_1, γ_2, and γ_3 are, respectively, obtained as $\gamma_1^u = \min\{\theta_1,\theta_2\}$, $\gamma_2^u = \min\{\rho_1,\theta_2\}$, and $\gamma_3^u = \min\{\theta_1,\rho_2\}$. Here, $\theta_1 = \beta_2 X_2/X_4$, $\theta_2 = \beta_1 X_1/X_3$, $\rho_1 = \beta_1 X_2/\beta_3$, and $\rho_2 = \beta_2 X_1/\beta_4$. Thus, the CDFs of γ_1^u, γ_2^u, and γ_3^u can be, respectively, obtained as

$$F_{\gamma_1^u}(\gamma) = 1 - [1-F_{\theta_1}(\gamma)][1-F_{\theta_2}(\gamma)] \quad (38)$$

$$F_{\gamma_2^u}(\gamma) = 1 - [1-F_{\rho_1}(\gamma)][1-F_{\theta_2}(\gamma)] \quad (39)$$

$$F_{\gamma_3^u}(\gamma) = 1 - [1-F_{\theta_1}(\gamma)][1-F_{\rho_2}(\gamma)] \quad (40)$$

where the CDFs of θ_1, θ_2, ρ_1, and ρ_2 are given by

$$F_{\theta_1}(\gamma) = \int_0^\infty F_{X_2}\left(\frac{\gamma x_4}{\beta_2}\right) f_{X_4}(x_4)\mathrm{d}x_4 \quad (41)$$

$$F_{\theta_2}(\gamma) = \int_0^{\infty} F_{X_1}\left(\frac{\gamma x_3}{\beta_1}\right) f_{X_3}(x_3)\mathrm{d}x_3 \tag{42}$$

$$F_{\rho_1}(\gamma) = F_{X_2}\left(\frac{\beta_3\gamma}{\beta_1}\right) \tag{43}$$

$$F_{\rho_2}(\gamma) = F_{X_1}\left(\frac{\beta_4\gamma}{\beta_2}\right) \tag{44}$$

Given $f_{X_i}(x_i)$ in (22) and $F_{X_i}(x_i)$ in (23), $i \in \{1,2,3,4\}$, followed by the help of [18, eq. (3.381.4)], we attain expressions for $F_{\theta_1}(\gamma)$, $F_{\theta_2}(\gamma)$, $F_{\rho_1}(\gamma)$, and $F_{\rho_2}(\gamma)$. Substituting these outcomes into (38)–(40), expressions for $F_{\gamma_1^u}(\gamma)$, $F_{\gamma_2^u}(\gamma)$, and $F_{\gamma_3^u}(\gamma)$ are found as

$$F_{\gamma_1^u}(\gamma) = 1 - \sum_{p=0}^{m_1-1}\sum_{q=0}^{m_2-1} \frac{1}{p!q!}\frac{\Gamma(m_3+p)\Gamma(m_4+q)\beta_1^{m_3}}{\Gamma(m_3)\Gamma(m_4)} \times \frac{\beta_2^{m_4}\alpha_3^{m_3}\alpha_4^{m_4}}{\alpha_1^{m_3}\alpha_2^{m_4}} \frac{\gamma^{p+q}}{\left(\gamma+\frac{\beta_1\alpha_3}{\alpha_1}\right)^{m_3+p}\left(\gamma+\frac{\beta_2\alpha_4}{\alpha_2}\right)^{m_4+q}} \tag{45}$$

$$F_{\gamma_2^u}(\gamma) = 1 - \sum_{q=0}^{m_2-1}\frac{1}{q!}\sum_{p=0}^{m_1-1}\frac{1}{p!}\frac{\Gamma(m_3+p)}{\Gamma(m_3)}\frac{\alpha_2^q\alpha_3^{m_3}\beta_1^{m_3-q}\beta_3^q}{\alpha_1^{m_3}} \times \frac{\gamma^{p+q}}{\left(\gamma+\frac{\beta_1\alpha_3}{\alpha_1}\right)^{m_3+p}}\exp\left(-\frac{\alpha_2\beta_3\gamma}{\beta_1}\right) \tag{46}$$

$$F_{\gamma_3^u}(\gamma) = 1 - \sum_{p=0}^{m_1-1}\frac{1}{p!}\sum_{q=0}^{m_2-1}\frac{1}{q!}\frac{\Gamma(m_4+q)}{\Gamma(m_4)}\frac{\beta_2^{m_4-p}\beta_4^p\alpha_1^p\alpha_4^{m_4}}{\alpha_2^{m_4}} \times \frac{\gamma^{p+q}}{\left(\gamma+\frac{\beta_2\alpha_4}{\alpha_2}\right)^{m_4+q}}\exp\left(-\frac{\alpha_1\beta_4\gamma}{\beta_2}\right) \tag{47}$$

Scenario 1: In order to compute the SER for Scenario 1, first, we replace $F_{\gamma_i}(\gamma)$ in (37) by $F_{\gamma_1^u}(\gamma)$ in (45). Then, we utilize [18, eq. (2.102)] to transform the integral expression into tabulated form. Finally, we apply [18, eq. (3.361.2)] and [29, eq. (2.3.6.9)] to calculate the resulting integrals that leads to an expression for the SER of the system for Scenario 1 as

$$\begin{aligned} P_{1,E} = \frac{a}{2} - \frac{a\sqrt{b}}{2\sqrt{\pi}}\sum_{p=0}^{m_1-1}\sum_{q=0}^{m_2-1}\frac{\Gamma(m_3+p)}{p!\,q!}\frac{\beta_1^{m_3}\beta_2^{m_4}\alpha_3^{m_3}\alpha_4^{m_4}}{\alpha_1^{m_3}\alpha_2^{m_4}} \times \frac{\Gamma(m_4+q)}{\Gamma(m_3)\Gamma(m_4)}\Gamma\left(p+q+\frac{1}{2}\right) \\ \times \left[\sum_{i=1}^{m_3+p}\kappa_{p,i}\left(\frac{\beta_1\alpha_3}{\alpha_1}\right)^{p+q-i+\frac{1}{2}} \times U\left(p+q+\frac{1}{2}, p+q-i+\frac{3}{2}, b\frac{\beta_1\alpha_3}{\alpha_1}\right)\right. \\ \left. + \sum_{j=1}^{m_4+q}\xi_{q,j}\left(\frac{\beta_2\alpha_4}{\alpha_2}\right)^{p+q-j+\frac{1}{2}} \times U\left(p+q+\frac{1}{2}, p+q-j+\frac{3}{2}, b\frac{\beta_2\alpha_4}{\alpha_2}\right)\right] \end{aligned} \tag{48}$$

where $\kappa_{p,i}$ and $\xi_{q,j}$ are partial fraction coefficients

$$\kappa_{p,i} = \frac{1}{(m_3+p-i)!}\left.\frac{d^{m_3+p-i}\left[\left(\gamma+\frac{\beta_2\alpha_4}{\alpha_2}\right)^{-m_4-q}\right]}{d\gamma^{m_3+p-i}}\right|_{\gamma=-\frac{\beta_1\alpha_3}{\alpha_1}}$$

$$\xi_{q,j} = \frac{1}{(m_4+q-j)!}\left.\frac{d^{m_4+q-j}\left[\left(\gamma+\frac{\beta_1\alpha_3}{\alpha_1}\right)^{-m_3-p}\right]}{d\gamma^{m_4+q-j}}\right|_{\gamma=-\frac{\beta_2\alpha_4}{\alpha_2}}$$

Scenario 2: By replacing $F_{\gamma_i}(\gamma)$ in (37) by $F_{\gamma_2^u}(\gamma)$ in (46), then making use of [18, eq. (3.361.2)] and [29, eq. (2.3.6.9)] to calculate the remaining integrals, an expression for the SER of Scenario 2 can be obtained as

$$P_{2,E} = \frac{a}{2} - \frac{a\sqrt{b}}{2\sqrt{\pi}}\sum_{q=0}^{m_2-1}\sum_{p=0}^{m_1-1}\frac{\beta_1^{\frac{1}{2}}\beta_3^q}{p!q!}\frac{\alpha_2^q\alpha_3^{q+\frac{1}{2}}}{\alpha_1^{q+\frac{1}{2}}}\frac{\Gamma\left(p+q+\frac{1}{2}\right)}{\Gamma(m_3)} \times \Gamma(m_3+p)U\left(p+q+\frac{1}{2}, q+\frac{3}{2}-m_3, \frac{\alpha_2\beta_3\alpha_3+\beta_1 b\alpha_3}{\alpha_1}\right) \tag{49}$$

Scenario 3: Similarly, the SER for Scenario 3 is given by

$$P_{3,E} = \frac{a}{2} - \frac{a\sqrt{b}}{2\sqrt{\pi}}\sum_{p=0}^{m_1-1}\sum_{q=0}^{m_2-1}\frac{1}{p!q!}\frac{\Gamma(m_4+q)\Gamma\left(p+q+\frac{1}{2}\right)\beta_2^{\frac{1}{2}}}{\Gamma(m_4)} \times \frac{\beta_4^p\alpha_1^p\alpha_4^{p+\frac{1}{2}}}{\alpha_2^{p+\frac{1}{2}}}U\left(p+q+\frac{1}{2}, p+\frac{3}{2}-m_4, \frac{\alpha_1\alpha_4\beta_4+\alpha_4\beta_2 b}{\alpha_2}\right) \tag{50}$$

Scenario 4: Finally, replacing $F_{\gamma_i}(\gamma)$ in (37) by $F_{\gamma_4}(\gamma)$ in (35), followed by using [18, eq. (3.361.2)] and [18, eq. (6.621.3)] to compute the resulting integrals, an expression for the SER of Scenario 4 can be given by

$$\begin{aligned} P_{4,E} = \frac{a}{2} - a\sqrt{b}\sum_{p=0}^{m_1-1}\frac{1}{p!}\sum_{q=0}^{p}\frac{C_q^p}{\Gamma(m_2)}\sum_{i=0}^{m_2-1}C_i^{m_2-1}4^{i-q+1} \\ \times \frac{\beta_5^{\frac{1}{2}}\Gamma\left(m_2+p+i-q+\frac{3}{2}\right)\Gamma\left(m_2+p+q-i-\frac{1}{2}\right)}{\left(\alpha_1+\alpha_2+b\,\beta_5+2\sqrt{\alpha_1\alpha_2}\right)^{m_2+p+i-q+\frac{3}{2}}} \\ \times \frac{\alpha_1^{p+i-q+1}\alpha_2^{m_2}}{\Gamma(m_2+p+1)} \\ \times {}_2F_1\left(m_2+p+i-q+\frac{3}{2}, i-q+\frac{3}{2}; \right. \\ \left. m_2+p+1; \frac{\alpha_1+\alpha_2+b\beta_5-2\sqrt{\alpha_1\alpha_2}}{\alpha_1+\alpha_2+b\beta_5+2\sqrt{\alpha_1\alpha_2}}\right) \end{aligned} \tag{51}$$

Now, we are ready to obtain the average SER of the system by substituting (48)–(51) into (36).

C. Outage Capacity Performance

Outage capacity C_ϵ in (bits/s/Hz) of the hybrid CCRN, i.e. the largest rate of transmission to guarantee that the outage probability is less than $\epsilon\%$, is derived from (25) as

$$C_\epsilon = \sum_{i=1}^{4} p_i C_{i,\epsilon} \tag{52}$$

where $C_{i,\epsilon}$, $i \in \{1,2,3,4\}$, is the outage capacity per unit bandwidth of Scenario i. In view of [30], a Gaussian approximation for the CDF of the channel capacity has been considered as an efficient method to evaluate outage capacity. Here, we apply the Gaussian approximation for the CDF of the channel capacity C_i of Scenario i as follows:

$$F_{C_i}(c) \approx 1 - \frac{1}{2}\mathrm{erfc}\left[\frac{c - E\{C_i\}}{\sqrt{2\left(E\{C_i^2\} - (E\{C_i\})^2\right)}}\right] \tag{53}$$

where $\mathrm{erfc}[\cdot]$ is the complementary error function. Furthermore, $E\{C_i\}$ and $E\{C_i^2\}$ are the first and the second moment of the channel capacity of Scenario i. As in [30], outage capacity $C_{i,\epsilon}$ of Scenario i corresponding to $\epsilon\%$ outage probability can be approximated from (53) as

$$C_{i,\epsilon} = E\{C_i\} + \sqrt{2\left(E\{C_i^2\} - (E\{C_i\})^2\right)}\mathrm{erfc}^{-1}\left[2 - \frac{\epsilon}{50}\right] \tag{54}$$

In order to derive the outage capacity of Scenario i, we need to obtain the first and the second moment of the channel capacity. Based on the Shannon capacity theorem, the instantaneous channel capacity in (bits/s/Hz) of Scenario i is expressed as

$$C_i = \frac{1}{2}\log_2(1+\gamma_i) = \frac{\ln(1+\gamma_i)}{2\ln 2} \tag{55}$$

Utilizing the Tayor series expansion of $\ln(1+\gamma_i)$ around the mean value $E\{\gamma_i\}$ of the effective SINR (or SNR in Scenario 4) γ_i, we have

$$\begin{aligned}\ln(1+\gamma_i) &= \ln(1+E\{\gamma_i\}) + \sum_{m=1}^{\infty}\frac{(-1)^{m-1}}{m}\frac{(\gamma_i - E\{\gamma_i\})^m}{(1+E\{\gamma_i\})^m} \\ &\approx \ln(1+E\{\gamma_i\}) + \frac{\gamma_i - E\{\gamma_i\}}{1+E\{\gamma_i\}} - \frac{1}{2}\frac{(\gamma_i - E\{\gamma_i\})^2}{(1+E\{\gamma_i\})^2}\end{aligned} \tag{56}$$

Applying the expectation operation for C_i and C_i^2, the second-order approximations for $E\{C_i\}$ and $E\{C_i^2\}$ are obtained as

$$E\{C_i\} \approx \frac{1}{2\ln 2}\left[\ln(1+E\{\gamma_i\}) - \frac{E\{\gamma_i^2\} - (E\{\gamma_i\})^2}{2(1+E\{\gamma_i\})^2}\right] \tag{57}$$

$$\begin{aligned}E\{C_i^2\} \approx \left(\frac{1}{2\ln 2}\right)^2\Bigg[&(\ln(1+E\{\gamma_i\}))^2 + \frac{E\{\gamma_i^2\} - (E\{\gamma_i\})^2}{(1+E\{\gamma_i\})^2} \\ &\times \ln\left(\frac{e}{1+E\{\gamma_i\}}\right)\Bigg]\end{aligned} \tag{58}$$

where e is the Napier constant and $E\{\gamma_i^n\}$, $n = 1, 2$, is the nth moment of the effective SINR (or SNR in Scenario 4) γ_i, i.e.,

$$E\{\gamma_i\} = \int_0^\infty \gamma f_{\gamma_i}(\gamma)\, d\gamma = \int_0^\infty [1 - F_{\gamma_i}(\gamma)]\, d\gamma \tag{59}$$

$$E\{\gamma_i^2\} = \int_0^\infty \gamma^2 f_{\gamma_i}(\gamma) d\gamma = 2\int_0^\infty \gamma\,[1 - F_{\gamma_i}(\gamma)]\, d\gamma \tag{60}$$

Again, it is noted that calculating $E\{\gamma_i\}$ and $E\{\gamma_i^2\}$ for Scenarios 1, 2, 3, and 4 directly from the exact expressions of the CDFs of γ_1 in (32), γ_2 in (33), γ_3 in (34), and γ_4 in (35) is intractable. Thus, $E\{\gamma_i\}$ and $E\{\gamma_i^2\}$ are computed from the CDF of the bound on γ_i, $i \in \{1,2,3,4\}$. The CDFs of the bounds on γ_1, γ_2, and γ_3 are derived in (45)–(47), respectively. Now, we need to derive the CDF of the bound on γ_4. Applying [27, eq. (25)] and [28, eq. (2)], from (21), the bound γ_4^u on the instantaneous SNR γ_4 can be found as

$$\gamma_4^u = \min(\chi_1, \chi_2) \tag{61}$$

where $\chi_1 = \beta_5 X_1$ and $\chi_2 = \beta_5 X_2$. Hence, an expression for the CDF of γ_4^u is given by

$$F_{\gamma_4^u}(\gamma) = 1 - [1 - F_{\chi_1}(\gamma)]\,[1 - F_{\chi_2}(\gamma)] \tag{62}$$

From (23) together with the help of [18, eq. (3.381.4)], we attain expressions for $F_{\chi_1}(\gamma)$ and $F_{\chi_2}(\gamma)$. With these outcomes, $F_{\gamma_4^u}(\gamma)$ is obtained as

$$F_{\gamma_4^u}(\gamma) = 1 - \sum_{p=0}^{m_1-1}\sum_{q=0}^{m_2-1}\frac{\alpha_1^p\alpha_2^q}{p!q!}\frac{\gamma^{p+q}}{\beta_5^{p+q}}\exp\left(-\frac{(\alpha_1+\alpha_2)\gamma}{\beta_5}\right) \tag{63}$$

Scenario 1: In order to calculate $E\{\gamma_1\}$ and $E\{\gamma_1^2\}$, we first replace $F_{\gamma_i}(\gamma)$ in (59) and (60) by $F_{\gamma_1^u}(\gamma)$ in (45). Then, taking advantage of [18, eq. (3.197.1)] to solve the resulting integrals, expressions for $E\{\gamma_1\}$ and $E\{\gamma_1^2\}$ are obtained as

$$\begin{aligned}E\{\gamma_1\} &= \sum_{p=0}^{m_1-1}\frac{1}{p!}\sum_{q=0}^{m_2-1}\frac{1}{q!}\frac{\Gamma(m_3+p)\Gamma(m_4+q)}{\Gamma(m_3)\Gamma(m_4)} \\ &\times \frac{\beta_2^{p+1}}{\beta_1^p\alpha_2^{p+1}\alpha_3^p}\alpha_1^p\alpha_4^{p+1}\mathcal{B}(p+q+1, m_3+m_4-1) \\ &\times {}_2F_1\left(m_3+p, p+q+1; m_3+p+m_4+q; 1-\frac{\beta_2\alpha_1\alpha_4}{\beta_1\alpha_2\alpha_3}\right)\end{aligned} \tag{64}$$

$$\begin{aligned}E\{\gamma_1^2\} &= 2\sum_{p=0}^{m_1-1}\frac{1}{p!}\sum_{q=0}^{m_2-1}\frac{1}{q!}\frac{\Gamma(m_3+p)\Gamma(m_4+q)}{\Gamma(m_3)\Gamma(m_4)} \\ &\times \frac{\beta_2^{p+2}}{\beta_1^p\alpha_2^{p+2}\alpha_3^p}\alpha_1^p\alpha_4^{p+2}\mathcal{B}(p+q+2, m_3+m_4-2) \\ &\times {}_2F_1\left(m_3+p, p+q+2; m_3+m_4+p+q; 1-\frac{\beta_2\alpha_1\alpha_4}{\beta_1\alpha_2\alpha_3}\right)\end{aligned} \tag{65}$$

Scenario 2: Replacing $F_{\gamma_i}(\gamma)$ in (59) by $F_{\gamma_2^u}(\gamma)$ in (46), then applying [29, eq. (2.3.6.9)] to handle the resulting integral, an expression for $E\{\gamma_2\}$ is given by

$$E\{\gamma_2\} = \sum_{p=0}^{m_1-1}\sum_{q=0}^{m_2-1} \frac{\beta_1\beta_3^q}{p!q!}\frac{\alpha_2^q\alpha_3^{q+1}}{\alpha_1^{q+1}}\frac{\Gamma(m_3+p)\Gamma(p+q+1)}{\Gamma(m_3)} \times U\left(p+q+1, q+2-m_3, \frac{\beta_3\alpha_2\alpha_3}{\alpha_1}\right) \quad (66)$$

Similarly, $E\{\gamma_2^2\}$ is obtained as

$$E\{\gamma_2^2\} = 2\sum_{p=0}^{m_1-1}\sum_{q=0}^{m_2-1} \frac{\beta_1^2\beta_3^q}{p!q!}\frac{\alpha_2^q\alpha_3^{q+2}}{\alpha_1^{q+2}}\frac{\Gamma(m_3+p)\Gamma(p+q+2)}{\Gamma(m_3)} \times U\left(p+q+2, q+3-m_3, \frac{\beta_3\alpha_2\alpha_3}{\alpha_1}\right) \quad (67)$$

Scenario 3: Utilizing the approach of calculating $E\{\gamma_2\}$ and $E\{\gamma_2^2\}$, expressions for $E\{\gamma_3\}$ and $E\{\gamma_3^2\}$ can be obtained as

$$E\{\gamma_3\} = \sum_{p=0}^{m_1-1}\sum_{q=0}^{m_2-1} \frac{\beta_2\beta_4^p}{p!q!}\frac{\alpha_1^p\alpha_4^{p+1}}{\alpha_2^{p+1}}\frac{\Gamma(m_4+q)\Gamma(p+q+1)}{\Gamma(m_4)} \times U\left(p+q+1, p+2-m_4, \frac{\alpha_1\alpha_4\beta_4}{\alpha_2}\right) \quad (68)$$

$$E\{\gamma_3^2\} = 2\sum_{p=0}^{m_1-1}\sum_{q=0}^{m_2-1} \frac{\beta_2^2\beta_4^p}{p!q!}\frac{\alpha_1^p\alpha_4^{p+2}}{\alpha_2^{p+2}}\frac{\Gamma(m_4+q)\Gamma(p+q+2)}{\Gamma(m_4)} \times U\left(p+q+2, p+3-m_4, \frac{\alpha_1\alpha_4\beta_4}{\alpha_2}\right) \quad (69)$$

Scenario 4: Finally, replacing $F_{\gamma_i}(\gamma)$ in (59) and (60) by $F_{\gamma_4^u}(\gamma)$ in (63), then utilizing [18, eq. (3.381.4)] to handle the resulting integrals, we obtain expressions for $E\{\gamma_4\}$ and $E\{\gamma_4^2\}$ as

$$E\{\gamma_4\} = \sum_{p=0}^{m_1-1}\sum_{q=0}^{m_2-1} \frac{\alpha_1^p\alpha_2^q\beta_5}{p!q!}\frac{\Gamma(p+q+1)}{(\alpha_1+\alpha_2)^{p+q+1}} \quad (70)$$

$$E\{\gamma_4^2\} = 2\sum_{p=0}^{m_1-1}\sum_{q=0}^{m_2-1} \frac{\alpha_1^p\alpha_2^q\beta_5^2}{p!q!}\frac{\Gamma(p+q+2)}{(\alpha_1+\alpha_2)^{p+q+2}} \quad (71)$$

By substituting $E\{\gamma_i\}$ and $E\{\gamma_i^2\}$ into (57) and (58), expressions for the mean $E\{C_i\}$ and second moment $E\{C_i^2\}$ of channel capacity of Scenario i are obtained. As a result, an expression for outage capacity $C_{i,\epsilon}$ of Scenario i can be easily attained by substituting these outcomes into (54) which leads to an expression for outage capacity C_ϵ of the system.

IV. Numerical Results

In this section, numerical results are provided to illustrate the impact of system parameters on the performance of the secondary network. For this purpose, we consider arrival rate of the primary network, average transmit SNR $P_{\max}/N_0$ of the secondary network in interweave mode, interference power threshold Q of the primary receiver, and distances from $\mathrm{S_S}$ to $\mathrm{P_D}$ and from $\mathrm{S_R}$ to $\mathrm{P_D}$. According to [31], [32], spectrum occupancy of the worldwide licensed users in the 25–3400 MHz frequency range is rather low. Specifically, in the range from 470 MHz to 766 MHz and from 880 MHz to 960 MHz, which are used for cellular phone networks, the average fraction of time that primary users utilize the licensed bands is highest with around 0.45. However, other frequency ranges are much lower utilized, e.g., occupancy ratio for the range from 960 MHz to 1525 MHz was only about 0.0236. As a result, the mean occupancy ratio over the whole range from 25 MHz to 3400 MHz was measured as 0.12 [32]. Thus, for the numerical examples, we select arrival rates and departure rates such that the probability for a primary transmission occurring $(p_p + p_{ps} + p_{pr})$ is less than 0.5. Let d_1, d_2, d_3, d_4, d_5, and d_6 denote the normalized distances from $\mathrm{S_S}$ to $\mathrm{S_R}$, $\mathrm{S_R}$ to $\mathrm{S_D}$, $\mathrm{S_S}$ to $\mathrm{P_D}$, $\mathrm{S_R}$ to $\mathrm{P_D}$, $\mathrm{P_S}$ to $\mathrm{S_R}$, and $\mathrm{P_S}$ to $\mathrm{S_D}$, respectively. Assume that channel mean powers are attenuated with distance according to the exponential decaying model with path-loss exponent $n = 4$ as for a suburban environment. The fading severity parameters are selected as $m_1 = m_2 = m_3 = m_4 = 3$. We approximate the effect of interference and noise at the relay and the secondary receiver as Gaussian variables n_r and n_d with zero-mean and variance N_r and N_d, respectively. Here, N_r and N_d are calculated based on the power law decaying path-loss as well as on the noise at the relay and the secondary receiver, i.e., $N_r = N_0 + d_5^{-n}P_p$ and $N_d = N_0 + d_6^{-n}P_p$ where P_p is the transmit power of $\mathrm{P_S}$. The SNR threshold to calculate the outage is fixed at $\gamma_{th} = 3$ dB and the outage probability threshold to calculate the outage capacity is chosen as $\epsilon = 1\%$.

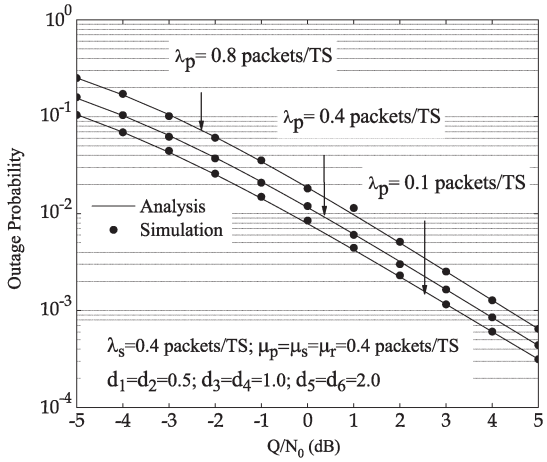

Fig. 3. Outage probability of a hybrid interweave-underlay CCRN versus interference power-to-noise ratio Q/N_0 for different arrival rates λ_p of the primary user.

Figs. 3–5, respectively, depict outage probability, SER, and outage capacity versus interference power-to-noise ratio Q/N_0 for various arrival rates λ_p at the primary transmitter. The average transmit SNR of the primary network and the secondary network in interweave mode are selected as $P_p/N_0 = 7$ dB and $P_{\max}/N_0 = 10$ dB. We assume that the arrival rate of the secondary network is $\lambda_s = 0.4$ packets/TS and that the departure rates of the secondary network and primary network are the same for all examples, i.e., $\mu_p = \mu_s = \mu_r = 0.4$ packets/TS. In an AF relay network, the departure rate of $\mathrm{S_S}$ becomes the

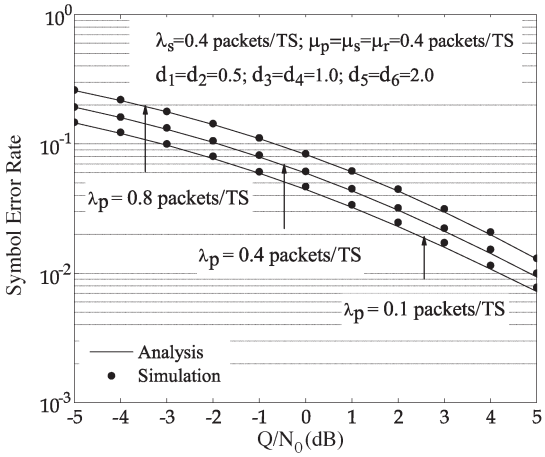

Fig. 4. SER of 8-PSK modulation for a hybrid interweave-underlay CCRN versus interference power-to-noise ratio Q/N_0 for different arrival rates λ_p of the primary user.

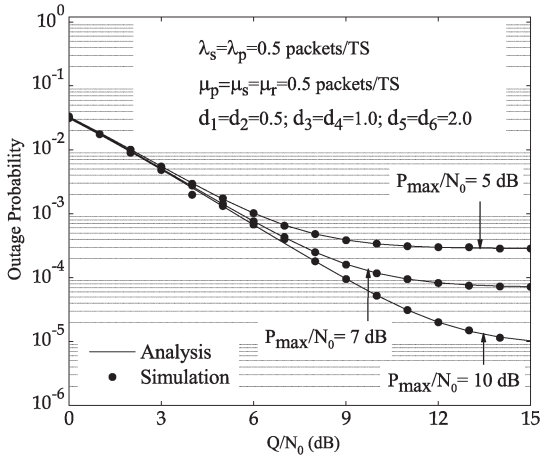

Fig. 6. Outage probability of a hybrid interweave-underlay CCRN versus interference power-to-noise ratio Q/N_0 for different average transmit SNRs $P_{\max}/N_0$ in interweave mode.

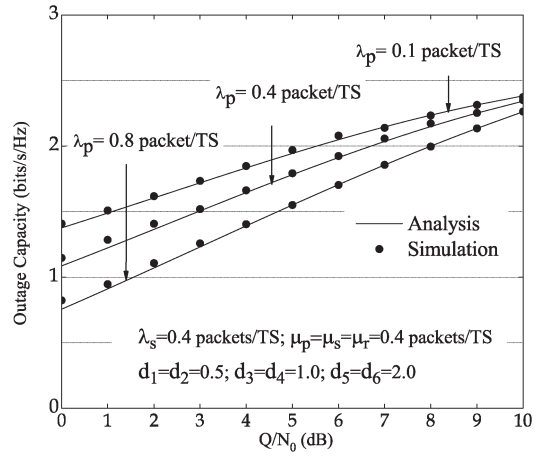

Fig. 5. Outage capacity for a hybrid interweave-underlay CCRN versus interference power-to-noise ratio Q/N_0 for different arrival rates λ_p of the primary user.

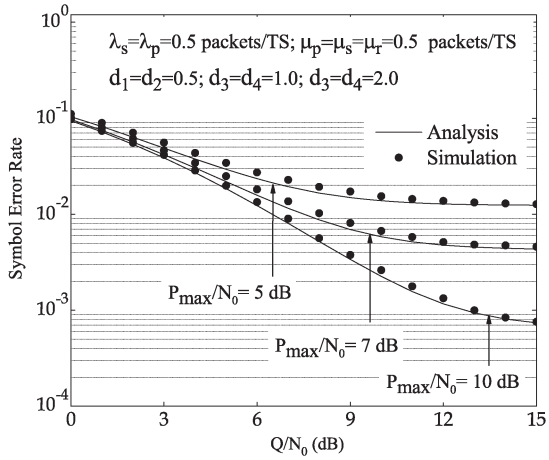

Fig. 7. SER of 8-PSK modulation for a hybrid interweave-underlay CCRN versus interference power-to-noise ratio Q/N_0 for different average transmit SNRs $P_{\max}/N_0$ in interweave mode.

arrival rate of $\mathrm{S_R}$, i.e., $\lambda_r = \mu_s$. For all examples of Figs. 3–5, the normalized distances are fixed as $d_1 = d_2 = 0.5$, $d_3 = d_4 = 1.0$, and $d_5 = d_6 = 2.0$. As expected, when the arrival rate of the primary network decreases, the performance of the hybrid system is improved. Specifically, outage probability and SER of the hybrid system decrease, and outage capacity increases. This is due to the fact that as λ_p decreases, the idle periods of the primary source increase. Thus, the probability that the CCRN operates in interweave mode without facing the interference constraint increases.

Figs. 6–8, respectively, illustrate outage probability, SER, and outage capacity versus interference power-to-noise ratio Q/N_0 for different values of average transmit SNR $P_{\max}/N_0$. The average transmit SNR of the primary network is selected as $P_p/N_0 = 7$ dB. Arrival rates and departure rates at the primary network and secondary network are selected as $\lambda_p = \lambda_s = 0.5$ packets/TS and $\mu_p = \mu_s = \mu_r = 0.5$ packets/TS. In addition, we fix $d_1 = d_2 = 0.5$, $d_3 = d_4 = 1.0$, and $d_5 = d_6 = 2.0$ for all examples in Figs. 6–8. As can be observed from these figures, outage probability, SER, and outage capacity are improved as average transmit SNR $P_{\max}/N_0$ increases. However, the effect of $P_{\max}/N_0$ on outage probability, SER, and outage capacity is insignificant for low values of Q/N_0. At high values of Q/N_0, the outage probability, SER, and outage capacity performance are remarkably enhanced when $P_{\max}/N_0$ increases. The reason for this behavior is that the performance of the hybrid system is not only affected by $P_{\max}/N_0$ but also by the interference threshold Q at $\mathrm{P_D}$. For high values of Q, since the secondary transmission often satisfies this interference constraint, the performance is mainly affected by $P_{\max}/N_0$. As a result, when the average transmit SNR $P_{\max}/N_0$ increases, the performance will improve accordingly.

Figs. 9–11, respectively, show comparisons between outage probability, SER, and outage capacity of the hybrid interweave-underlay CCRN and that of the conventional underlay cognitive relay network. To make a fair comparison, in the examples, the parameters of the hybrid and underlay relay networks are chosen the same. Specifically, we fix the normalized transmission distances $d_1 = d_2 = 0.5$, $d_3 = d_4 = 1.0$ and vary distances d_5 and d_6. Furthermore, we select arrival rates and departure rates at the primary network and secondary network, respectively, as $\lambda_p = \lambda_s = 0.5$ packets/TS and $\mu_p = \mu_s = \mu_r = 0.2$

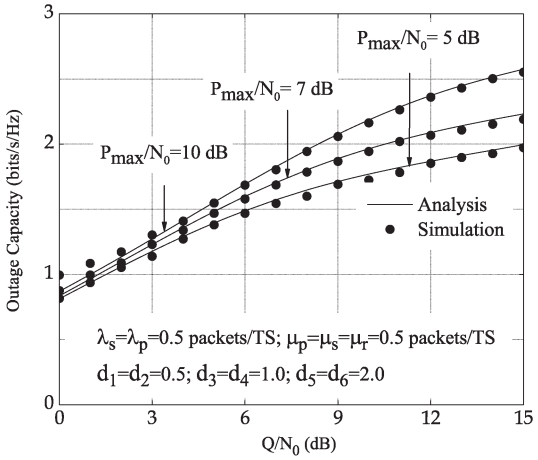

Fig. 8. Outage capacity for a hybrid interweave-underlay CCRN versus interference power-to-noise ratio Q/N_0 for different average transmit SNRs $P_{\max}/N_0$ in interweave mode.

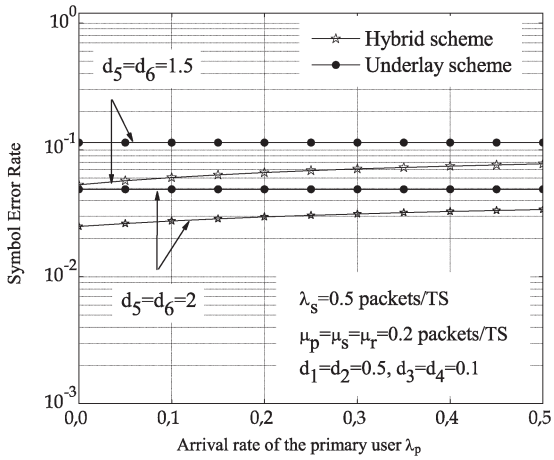

Fig. 10. Comparison of SER of 8-PSK modulation for underlay CCRN and hybrid interweave-underlay CCRN for different distances d_5 and d_6, respectively, from $\mathrm{P_S}$ to $\mathrm{S_R}$ and from $\mathrm{P_S}$ to $\mathrm{S_D}$.

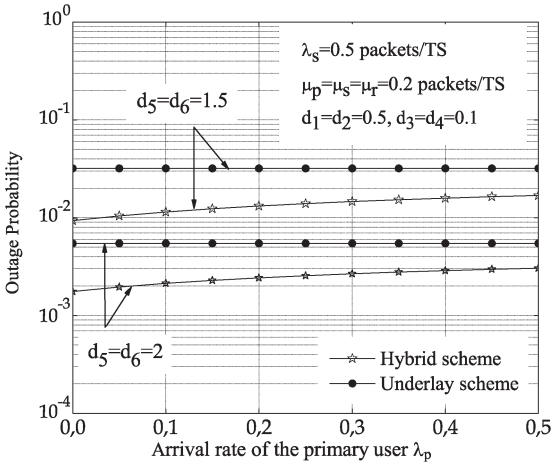

Fig. 9. Comparison of outage probability for underlay CCRN and hybrid interweave-underlay CCRN for different distances d_5 and d_6, respectively, from $\mathrm{P_S}$ to $\mathrm{S_R}$ and from $\mathrm{P_S}$ to $\mathrm{S_D}$.

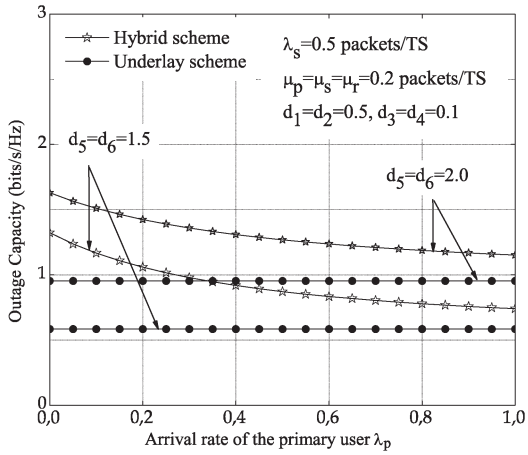

Fig. 11. Comparison of outage capacity for underlay CCRN and hybrid interweave-underlay CCRN for different distances d_5 and d_6, respectively, from $\mathrm{P_S}$ to $\mathrm{S_R}$ and from $\mathrm{P_S}$ to $\mathrm{S_D}$.

packets/TS. Finally, the average transmit SNR of the primary network and the secondary network in interweave mode and the interference power-to-noise ratio in underlay mode are selected as $P_p/N_0 = 7$ dB, $P_{\max}/N_0 = 10$ dB, and $Q/N_0 = 5$ dB in all examples. As expected, when the distances d_5 ($\mathrm{P_S}$ to $\mathrm{S_R}$) and d_6 ($\mathrm{P_S}$ to $\mathrm{S_D}$) increase, outage probability and SER decrease while outage capacity increases for both the hybrid scheme and the conventional cognitive scheme. This is because when the distances from $\mathrm{P_S}$ to $\mathrm{S_R}$ and $\mathrm{P_S}$ to $\mathrm{S_D}$ become larger, interference power from the primary transmitter to the secondary network becomes smaller. Furthermore, it can be observed that when the arrival rate of the primary network increases, the performance of the hybrid CCRN degrades but still outperforms the underlay scheme. However, the performance of the conventional underlay CCRN does not depend on the arrival rate of the primary network. This is because the underlay CCRN utilizes always only one spectrum access mode while the hybrid CCRN can adapt its spectrum access mode based on the state of the primary user.

More importantly, it can be seen from Figs. 9–11 that the performance of the hybrid CCRN always outperforms that of the conventional underlay CCRN with the same transmission distances, fading conditions, arrival and departure rates. This is because the secondary users in the hybrid CCRN can operate with maximum transmit power $P_{\max}$ when the primary transmission is idle. The secondary users only control their transmit powers when the primary transmission is active. On the contrary, in the conventional underlay CCRN, the secondary users always adjust their powers to satisfy the interference power constraint of the primary receiver, even when the primary transmission is idle. In case that the secondary network is located closely to the primary receiver, the transmit power of the conventional underlay CCRN is constrained to be much lower than its maximum transmit power $P_{\max}$ which leads to performance degradation as compared to the hybrid CCRN.

V. Conclusion

In this paper, we have studied a hybrid interweave-underlay spectrum access system with relaying transmission as a means of improving system performance. A continuous-time Markov

chain for modeling and analyzing the spectrum access mechanism of this hybrid CCRN has been developed. Upon the proposed Markov model, the steady-state probability of each state of the hybrid network has been obtained. This has enabled us to further develop a rigorous mathematical framework for performance analysis of such a system. In particular, we have assessed system performance in terms of outage probability, SER, and outage capacity over Nakagami-m fading by deriving the respective analytical expressions. The numerical results illustrate the effect of system parameters such as primary network arrival rate, distances from the PU to the SUs, interference power threshold of the underlay scheme, and average transmit SNR in interweave mode on the performance of the hybrid CCRN. Finally, the numerical results have also shown that the hybrid approach outperforms the conventional underlay scheme for the settings considered.

REFERENCES

[1] M. A. McHenry, "Spectrum white space measurements," presented at the New America Foundation Broadband Forum, Washington, DC, USA, Jun. 2003.

[2] J. M. Peha, "Approaches to spectrum sharing," *IEEE Commun. Mag.*, vol. 43, no. 2, pp. 10–12, Feb. 2005.

[3] S. Haykin, "Cognitive radio: Brain-empowered wireless communications," *IEEE J. Sel. Areas Commun.*, vol. 23, no. 2, pp. 201–220, Feb. 2005.

[4] R. Zhang, "On peak versus average interference power constraints for protecting primary users in cognitive radio networks," *IEEE Trans. Wireless Commun.*, vol. 8, no. 4, pp. 2112–2120, Apr. 2009.

[5] Y. C. Liang, Y. Zeng, E. C. Y. Peh, and A. Hoang, "Sensing-throughput tradeoff for cognitive radio networks," *IEEE Trans. Wireless Commun.*, vol. 7, no. 4, pp. 1326–1337, Apr. 2008.

[6] V. A. Bohara, S. H. Ting, Y. Han, and A. Pandharipande, "Interference-free overlay cognitive radio network based on cooperative space time coding," in *Proc. Cognit. Radio Oriented Wireless Netw. Commun.*, Cannes, France, Jun. 2010, pp. 1–5.

[7] W. Y. Lee and I. F. Akyildiz, "Optimal spectrum sensing framework for cognitive radio networks," *IEEE Trans. Wireless Commun.*, vol. 7, no. 10, pp. 3845–3857, Oct. 2008.

[8] A. Goldsmith, S. A. Jafar, I. Marić, and S. Srinivasa, "Breaking spectrum gridlock with cognitive radios: An information theoretic perspective," *Proc. IEEE*, vol. 97, no. 5, pp. 894–914, May 2009.

[9] Y. Xing, R. Chandramouli, S. Mangold, and S. S. Nandagopalan, "Dynamic spectrum access in open spectrum wireless networks," *IEEE J. Sel. Areas Commun.*, vol. 24, no. 3, pp. 626–637, Mar. 2006.

[10] J. Hu, L.-L. Yang, and L. Hanzo, "Optimal queue scheduling for hybrid cognitive radio maintaining maximum average service rate under delay constraint," in *Proc. IEEE Global Commun. Conf.*, Anaheim, CA, USA, Dec. 2012, pp. 1398–1403.

[11] K. B. S. Manosha, N. Rajatheva, and M. Latva-aho, "Overlay/underlay spectrum sharing for multi-operator environment in cognitive radio networks," in *Proc. IEEE Veh. Technol. Conf.*, Budapest, Hungary, May 2011, pp. 1–5.

[12] Q. Zhang, J. Jia, and J. Zhang, "Cooperative relay to improve diversity in cognitive radio networks," *IEEE Commun. Mag.*, vol. 47, no. 2, pp. 111–117, Feb. 2009.

[13] X. Gong, W. Yuan, W. Liu, W. Cheng, and S. Wang, "A cooperative relay scheme for secondary communication in cognitive radio networks," in *Proc. IEEE Global Commun. Conf.*, New Orleans, LA, USA, Dec. 2008, pp. 1–6.

[14] G. Zhao, C. Yang, G. Y. Li, D. Li, and A. C. K. Soong, "Power and channel allocation for cooperative relay in cognitive radio networks," *IEEE J. Sel. Topics Signal Process*, vol. 5, no. 1, pp. 151–159, Feb. 2011.

[15] S. Chen, W. Wang, and X. Zhang, "Performance analysis of multiuser diversity in cooperative multi-relay networks under Rayleigh-fading channels," *IEEE Trans. Wireless Commun.*, vol. 8, no. 7, pp. 3415–3419, Jul. 2009.

[16] Z. Yan, X. Zhang, and W. Wang, "Outage performance of relay assisted hybrid overlay/underlay cognitive radio systems," in *Proc. IEEE Wireless Commun. Netw. Conf.*, Quintana Roo, Mexico, Mar. 2011, pp. 1920–1925.

[17] B. Wang, Z. Ji, K. J. R. Liu, and T. Clancy, "Primary-prioritized Markov approach for dynamic spectrum allocation," *IEEE Trans. Wireless Commun.*, vol. 8, no. 4, pp. 1854–1865, Apr. 2009.

[18] I. S. Gradshteyn and I. M. Ryzhik, *Table of Integrals, Series, and Products,* 7th ed. New York, NY, USA: Academic, 2007.

[19] X. Kang, Y. C. Liang, H. K. Garg, and L. Zhang, "Sensing-based spectrum sharing in cognitive radio networks," *IEEE Trans. Veh. Technol.*, vol. 58, no. 8, pp. 4649–4654, Oct. 2009.

[20] L. Musavian, S. Aissa, and S. Lambotharan, "Effective capacity for interference and delay constrained cognitive radio relay channels," *IEEE Trans. Wireless Commun.*, vol. 9, no. 5, pp. 1698–1707, May 2010.

[21] Z. Shu, J. Zhou, Y. Yang, H. Sharif, and Y. Qian, "Network coding-aware channel allocation and routing in cognitive radio networks," in *Proc. IEEE Global Commun. Conf.*, Anaheim, CA, USA, Dec. 2012, pp. 5590–5595.

[22] H. Hu and Q. Zhu, "Dynamic spectrum access in underlay cognitive radio system with SINR constraints," in *Proc. IEEE Int. Conf. Wireless Communic., Netw. Mobile Comput.*, Beijing, China, Sep. 2009, pp. 1–4.

[23] W. J. Stewart, *Probability, Markov Chains, Queues, and Simulation: The Mathematical Basis of Performance Modeling*. Princeton, NJ, USA: Princeton Univ. Press, 2009.

[24] M. Aljuaid and H. Yanikomeroglu, "Investigating the Gaussian convergence of the distribution of the aggregate interference power in large wireless networks," *IEEE Trans. Veh. Technol.*, vol. 59, no. 9, pp. 4418–4424, Nov. 2010.

[25] H. Inaltekin, "Gaussian approximation for the wireless multi-access interference distribution," *IEEE Trans. Signal Process.*, vol. 60, no. 11, pp. 6114–6120, Nov. 2012.

[26] R. H. Y. Louie, Y. Li, H. A. Suraweera, and B. Vucetic, "Performance analysis of beamforming in two hop amplify and forward relay networks with antenna correlation," *IEEE Trans. Wireless Commun.*, vol. 8, no. 6, pp. 3132–3141, Jun. 2009.

[27] M. D. Renzo, F. Graziosi, and F. Santucci, "A comprehensive framework for performance analysis of dual-hop cooperative wireless systems with fixed-gain relays over generalized fading channels," *IEEE Trans. Wireless Commun.*, vol. 8, no. 10, pp. 5060–5074, Oct. 2009.

[28] S. Ikki and M. H. Ahmed, "Performance analysis of cooperative diversity wireless networks over Nakagami-m fading channel," *IEEE Commun. Lett.*, vol. 11, pp. 334–336, Jul. 2007.

[29] A. P. Prudnikov, Y. A. Brychkov, and O. I. Marichev, *Integrals and Series*, vol. 1. New York, NY, USA: Gordon and Breach, 1986.

[30] J. Perez, J. Ibanez, L. Vielva, and L. Santamariax, "Closed-form approximation for the outage capacity of orthogonal STBC," *IEEE Commun. Lett.*, vol. 9, no. 11, pp. 961–963, Nov. 2005.

[31] M. A. McHenry, "NSF spectrum occupancy measurements project summary," Shared Spectrum Company, Vienna, VA, USA, Aug. 2005.

[32] A. Martian, I. Marcu, and I. Marghescu, "Spectrum occupancy in an urban environment: A cognitive radio approach," in *Proc. Adv. Int. Conf. Telecommun.*, Barcelona, Spain, May 2010, pp. 25–29.

Thi My Chinh Chu was born in Ninh Binh, Vietnam, in November 1981. She received the B.S. and M.Sc. degrees in electronics and communications from Hanoi University of Technology, Hanoi, Vietnam, in 2004 and 2007, respectively. Since 2004, she has been with the Radio Broadcasting of Vietnam, the Voice of Vietnam (VOV). In April 2011, she joined the Radio Communications Group, Blekinge Institute of Technology, Karlskrona, Sweden as a Ph.D. candidate. Her current research interests include cooperative communications, cognitive radio networks, and combining cooperative diversity techniques into cognitive radio networks.

Hoc Phan received the B.S. degree in electronics and computer engineering from Da Nang University of Technology, Da Nang, Vietnam, in 2001; the M.S. degree in geographic information systems and the M.S. degree in electrical and electronics engineering from Ho Chi Minh University of Technology, Ho Chi Minh, Vietnam, in 2005 and 2006, respectively; and the Ph.D. degree in telecommunication systems from Blekinge Institute of Technology, Karlskrona, Sweden, in 2013. In May 2005, he joined the Department of Electrical, Electronics, and Telecommunications, Ho Chi Minh University of Transport, Ho Chi Minh. He is currently a Postdoctoral Research Associate with the University of Reading, Berkshire, U.K. His current research interests include cooperative communications, relay networks, cognitive radio networks, and network coding.

Hans-Jürgen Zepernick (M'94–SM'11) received the Dipl.-Ing. degree from the University of Siegen, Siegen, Germany, in 1987 and the Dr.-Ing. degree from the University of Hagen, Hagen, Germany, in 1994. From 1987 to 1989, he was with Siemens AG, Munich, Germany. He is currently a Professor of radio communications with the Blekinge Institute of Technology, Karlskrona, Sweden. Prior to this appointment, he was a Professor of wireless communications with Curtin University of Technology, Bentley, Australia; the Deputy Director of the Australian Telecommunications Research Institute, Perth, Australia; and an Associate Director of the Australian Telecommunications Cooperative Research Centre. His current research interests include cooperative communications, cognitive radio networks, mobile multimedia, and perceptual quality assessment.